



Antibacterial activities of layer double hydroxide nanocubes based on Zeolite templates and its high performance as a disinfectant

Moftah Essa Elkartehi^a, Amal Zaher^{a*}, Ahmed Farghali^b, Marzouk M. A^c, Rehab Mahmoud^d
Nabila Shehata^a

^a Department of environmental science and industrial development, Faculty of Postgraduate Studies for Advanced Sciences, Beni-Suef University, 62511 Beni-Suef, Egypt

^b Materials Science and Nanotechnology Department, Faculty of Postgraduate Studies for Advanced Sciences, Beni-Suef University

^c Botany and microbiology department, Faculty of Science, Beni-Suef University, 62511 Beni-Suef, Egypt.

^d Department of Chemistry, Faculty of Science, Beni-Suef University, 62511 Beni-Suef, Egypt.



CrossMark

Abstract

Inorganic metal oxides represent a class of materials that have been used for health applications. In this work, three nanomaterials were synthesized and characterized. Furthermore, the antibacterial activity of the synthesized materials was evaluated against the gram-negative bacterial species *Escherichia coli* and the gram-positive bacterial species *Staphylococcus aureus*, by using three materials the natural clay (Zeolite), Novel Zn-LDHs-modified zeolites and LDH-zeolite composite which was investigated using X-ray diffraction (XRD), Fourier transform infrared (FTIR) spectroscopy, and scanning electron microscope (SEM). The results of this study have shown that the antimicrobial activity measurement revealed that the LDH-zeolite composite exhibited more activity in gram-negative bacteria than gram-positive.

Keywords: Layer double hydroxide (LDH); nanocubes; disinfection; antimicrobial activity

1. Introduction

Layered Double Hydroxides (LDHs) are natural anionic clays it can be synthesized with economic and simple methods in laboratory. It has characteristic properties like high anionic exchange capacities, physical, chemical, effective biological properties, and large surface areas. Nowadays, the several applications of LDH in various fields such as catalysis, medical science, and separation technology have been investigated, due to the properties of LDH which include the open structure that can host a large range of anionic molecules, interlayer space, and adjustable textural properties. All these properties can be controlled by the condition of LDH synthesis [1–3]. The intensive application of antibiotics for veterinary, human, and agricultural purposes, results in their continuous release into environment [4–6]. The release of antibiotics into the ecosystem leads to develop the antibiotic resistance genes (ARGs), which reduce the therapeutic potential against pathogens in animals and humans. For this reason, researchers are interested to investigate the new and effective antibacterial agents [7] Inorganic metal

oxide nanoparticles such as LDHS have recently received great attention due to their specific properties [8–11]. The ability to prepare LDHS is likely lead to develop the new antibacterial agents. In this work, the three nano-materials have been applied as antibacterial materials. The first material was layered double hydroxides constitute (LDHs), the second applied material was Zeolites which naturally occurring porous crystalline aluminosilicate with three-dimensional structures and the third material was LDH-zeolite composite. All synthesized compounds have exhibited the antibacterial activity against Gram-positive bacteria, gram-negative bacteria, and a fungal strain (*Candida albicans* ATCC 60913).

2. Experimental Details

2.1. Materials

Zn(NO₃)₂·6H₂O (Chem-Lab NV, Belgium), Fe(NO₃)₃·9H₂O, HCl (Carlo Erba reagent), and NaOH (Piochem for laboratory chemicals, Egypt) were implemented without further purification. The preparations of the materials and the experimental

*Corresponding author e-mail: amal_2006z@yahoo.com (Amal Zaher)

Receive Date: 17 March 2022, Revise Date: 08 June 2022, Accept Date: 20 June 2022

DOI: 10.21608/EJCHEM.2022.128076.5679

©2023 National Information and Documentation Center (NIDOC)

assays were performed using deionized water free of CO₂.

2.2. Methods

2.2.1. Synthesis of ZnFe LDH

Co-precipitation, a traditional synthesis method was implemented for the ZnFe LDH preparation. Solutions of iron and zinc in the form of nitrate precursors were mixed in a molar ratio of 1:4. NaOH solution (2M) was introduced slowly, at 0.10 ml/min, until pH reaches 10 to ensure complete precipitation. The resulting product was aged at 333±0.5 K for 12 h; after that, the obtained material was filtered and washed many times with the aid of distilled water to get rid of excess alkalinity (OH⁻), followed by ethanol washing. In the end, the product was dried at 353±0.5K for 1d [12].

Zeolite nanoparticles were developed by processing the commercial zeolite in a photon ball milling vessel at a natural zeolite: balls mass ratio equal to 1:10, for 10 h, under a continuous mechanical rotation speed of 200 rpm. The balls and the vessel are constructed from porcelain and stain steel, respectively.

The nano-zeolite@FeZn LDH composite with a zeolite: Fe : Zn molar ratio equal to 0.5:1:4 was synthesized via introducing a Zeolite slurry (30 gm of Zeolite dissolved in 1L of bi-distilled water) to the reaction medium before precipitation under alkaline conditions (pH 8.0). The nano-zeolite@FeZn LDH suspension was mixed at room temperature for around 20 h, and then the composite precipitate was separated from the solution by filtration. The developed nanocomposite was subject to washing using bi-distilled water and ethanol many times and finally dried at 323K overnight.

2.3. Characterizations of the developed materials

The formed FeZn LDH, Zeolite nanoparticles and nano-zeolite@FeZn LDH composite were investigated by XRD (PANalytical Empyrean, Sweden) diffractometer. The operating conditions were: (1) an accelerating voltage of 40 KV, scan step 0.05°, scan angle (50 - 60°), and current 30 mA. The vibration kind and intensity of the chemical bonds were detected using a (vertex 70 FTIR-FT Raman: serial number 1341) Bruker instrument. It covered a wide frequency range (400- 4000 cm⁻¹) using a potassium bromide based disc. The morphology and molar ratio for each material was investigated using a Field Emission Scanning Electron Microscope and EDAX (Quanta FEG250, Germany) re-spectively. High-resolution transmission electron microscopy (HRTEM, JEOL-JEM 2100) was applied to investigate the microstructures of the synthesized materials. The surface areas and characteristics (pore size distribution, and pore volume) were estimated by N₂ adsorption isotherms using TriStar II 3020, Micrometrics, surface analyzer (USA). X-ray

photoelectron spectroscopy. The zeta potential and hydrodynamic particle size were determined using a Nano-Zeta sizer (Malvern Instruments Ltd, United Kingdom).

2.4 In-vitro antimicrobial activity

2.4.1 Microbial pathogens

Gram-positive bacteria (Staphylococcus aureus ATCC 43300, Sarcinalutea AOE, and Listeria monocytogenes ATCC 7644) and gram-negative bacteria (Escherichia coli ATCC 6933, Salmonella typhi ATCC 14028 and Pseudomonas auroginosa ATCC 9027) and a fungal strain (Candida albicans ATCC 60913).

2.4.2 Antimicrobial activity test

Antimicrobial sensitivity test using the agar diffusion method was applied and the minimum inhibitory concentration was evaluated where each overnight culture of the tested microorganisms (pathogens) was mixed with Muller Hinton agar media to give a final concentration of 1% microorganism (about 0.5 McFarland) and poured into sterile Petri dishes in a fixed amount of 20 mL using aseptic conditions. The sterile corkborer was used to prepare cups of 10 mm diameter. Test samples and standard drugs with volumes of 60 µL were introduced into cups with the help of a micropipette. All the plates were kept at room temperature for effective diffusion of the test drug and standard and incubated at 37 ± 1°C for 24 h. The presence of inhibition zones around the cup indicated antimicrobial activity. The diameter of the zone of inhibition was measured and recorded. A dose response curve was prepared based on plotting log concentrations of nanoparticles versus diameters of inhibition zone around the cups and the linear regression equations were generated to calculate MICs (The minimum inhibitory concentration) which is the lowest concentration causing complete inhibition of growth.

3. Results and discussion

3.1 Discussion of characterization results

The X-ray patterns of the developed sorbents are represented in Figure. (1-a). The XRD pattern of the prepared FeZn LDH agreed with that investigated in the literature [13], showing a well-organized layered pattern. The reflection peaks at 60.9°, 59.9°, 46.5°, 39.1°, 34.5°, 22.2°, and 11.6° could be referred to the plane families (0015), (110), (018), (015), (012), (006) and (003), respectively [14]. The significant peaks of LDH are confirmed as a broad peak in the range 11.6 - 22.2° as well as an intense peak at 34.5° while that characteristic of the zeolitic materials is located at 2θ values of 30°, 27.2°, 24°, and 21.7° Figure (1-a) [15,16]. For the nanocomposite, after zeolite loading, as shown in Figure (1-a), the peaks at the (006) and (003) faces disappeared which confirms the successful synthesis of the FeZn LDH as well as

the composite [14]. On the other hand, a significant diffraction peak of Zeolite at 27.2° disappeared in the composite pattern which is owed to the overlapping with another peak with high intensity referred to the FeZn LDH. Also, after the loading of zeolite into the FeZn LDH, the peaks intensities became higher, suggesting a crystallization of a higher degree for the zeolite@FeZn LDH compared to that of FeZn LDH [14,17]. Furthermore, some peaks were shifted, e.g., 36.46 to 36.47 , 31.96 to 31.98 , and 22.2 to 22.56° , while other peaks still stable (Fig. 1a). The crystalline sizes of zeolite nanoparticles, FeZn LDH and nano-zeolite@FeZn LDH were 40.21 , 35.10 , and 50.35 nm, respectively, which confirms the formation of the materials in the nanoscale. The peak at (003) disappearance refers to the transformation of the nanocomposite morphology from layered- into a cube-like structure. The HRTEM images shown in Figures 1b and 1c reveal that the layered structure of LDH and the shaded hexagonal structures of nano-zeolite@FeZn LDH.

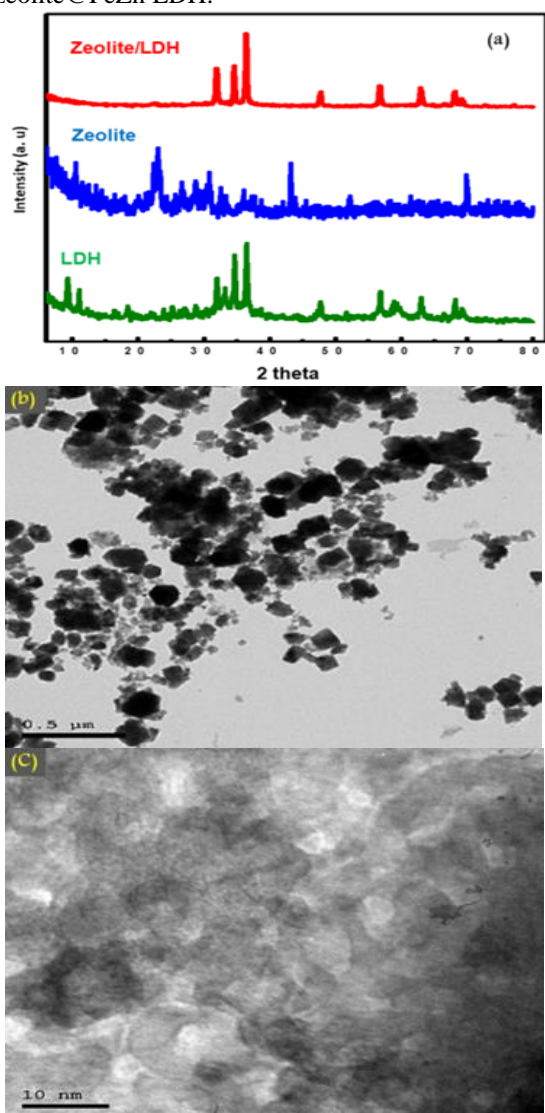


Figure (1) (a): XRD patterns of the synthesized sorbents, (b): HRTEM photos of nano-zeolite@FeZn LDH and (c): FeZn LDH.

The FT-IR spectrum of FeZn LDH Figure(2) shows a significant band at 1357 cm^{-1} referred to the existence of NO_3^- group. The OH^- group, in stretching mode, which confirms the presence of water molecules in the interlayer space of FeZn LDH yields a broad peak at 3400 cm^{-1} and a sharp peak at 1650 cm^{-1} . The broad one may be attributed to the presence of hydrogen bonds on the FeZn LDH surface [18]. The characteristic bending and stretching modes of Fe–O and Zn–O bonds are confirmed with the appearance of the bands in the range of 1000 cm^{-1} - 400 cm^{-1} [15]. In the spectra of nano-zeolite@FeZn LDH and zeolite (Fig. 2), a clear band at 3490 cm^{-1} was owned to the Si–OH and Al–OH groups onto the surface of zeolite [18]. A considerable band, at 1045 cm^{-1} , is referred to the stretching vibration of X–O where X is refers to Al or Si [19]. The presence of water molecules in zeolite was emphasized with different absorption bands where the bands at 1630 cm^{-1} and 3400 cm^{-1} refer to the bending mode of water and the O–H–O vibration [20]. The O–Si–O and O–Al–O bonds in the mode of bending vibration appear at 437 cm^{-1} [18]. The different bands at the wavenumber ranged from 500 cm^{-1} to 800 cm^{-1} owned to the pseudo-lattice vibrations, they also represent the characteristics of the channel cations [20]. These spectra are evidence on the synthesis of the nano-zeolite@FeZn LDH composite.

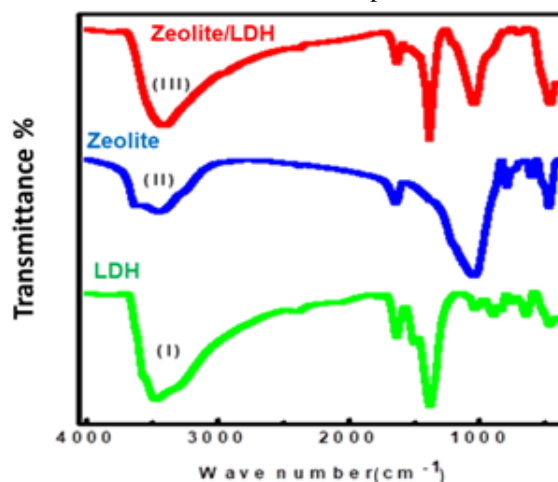
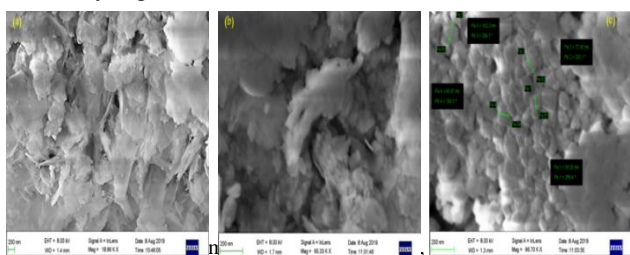


Figure (2) FTIR spectra of patterns of the three syntheses sorbents.

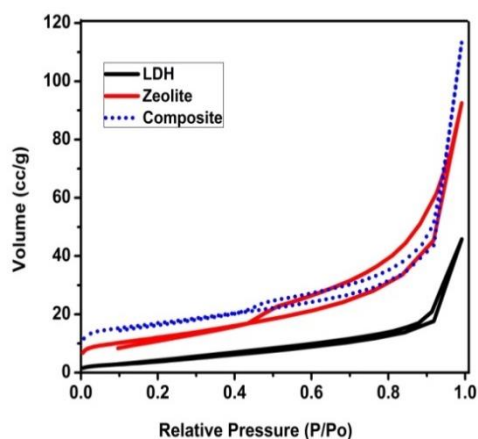
FE-SEM Figure (3) represents the morphologies of the synthesized materials. The FeZn LDH nanostructure is close to the shape of homogenous flakes located on each other, zeolite appears as a plane-like crystal surface adhered to each other and it is difficult to identify their crystallinity. On the other hand, nano-zeolite@FeZn LDH shows a well-defined cubic structure [21]. The transformation in the shape of the precursors (FeZn LDH and zeolite nanoparticles) from the flakes and crystals to the cubic shape (Figure (3-c)) may be interpreted to that the zeolite acted as a structural controlling agent by

the development of the complicated structure. It can be stacked on defined crystal planes of zones where the layer grows in certain directions.



nanoparticles and (c): nano-zeolite@FeZn LDH.

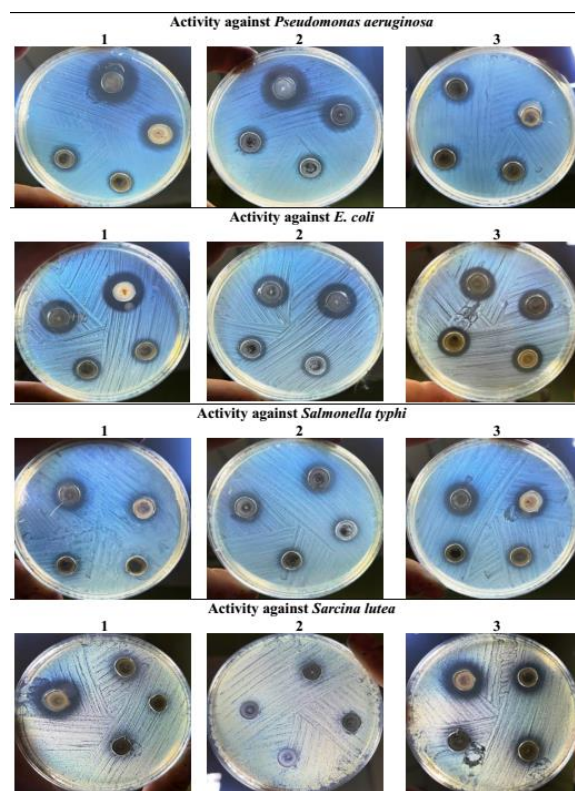
Figure (4) represents the N₂ adsorption/desorption isotherms at 77 K onto the materials under study. According to the International Union of Pure and Applied Chemistry (IUPAC) classification, all isotherms of FeZn LDH, zeolite nanoparticles, and nano-zeolite@LDH composite are of IV-type. Additionally, the stacking of the adsorption and desorption curves at the region P/P₀ < 0.40 refers to the presence of micropores. A relative pressure from 0.40 to 0.95, the hysteresis loop in zeolite nanoparticles is wider than that of FeZn LDH, which refers to that zeolite contains a larger amount of mesopores than does LDH. The specific surface areas of the zeolite nanoparticles, FeZn LDH, and nano-zeolite@FeZn LDH composite were 59.83, 16.85, and 55.94 m²/g, respectively. It can be concluded that the characteristics of composite surfaces arise from the surface characteristics of nano-zeolite. The total pore volumes of the zeolite nanoparticles, FeZn LDH, nano-zeolite@LDH are 0.15, 0.07 and 0.018 cc/g.



5.2. Antimicrobial investigation

Data shown in Figure (6) and Table 1 revealed that the gram-ve rods (*Pseudomonas aeruginosa*, *Escherichia coli*, and *Salmonella typhi*) were inhibited by the three nanoparticles samples (FeZn LDH, zeolite nanoparticles, and nano-zeolite@LDH nanocomposite). The diameter of the inhibition zone varied from 0 to 22 mm, this wide range in the pathogen inhibition was mainly induced by sample

LDH while samples zeolite nanoparticles and nano-zeolite@LDH could only stop the pathogen growth. Data also showed that there is a gradual increase in inhibition with increasing the concentration of the tested samples, where the maximum growth inhibition in the case of *Pseudomonas aeruginosa* was induced by LDH and zeolite nanoparticles at a concentration of 1000 ug/l (22mm) and in case of *Escherichia coli* the maximum inhibition was induced by LDH at a concentration of 1000ug/l (19mm) while in case of *Salmonella typhi* the maximum inhibition was induced by sample nano-zeolite@LDH at a concentration of 1000ug/l (17mm). The same pattern was detected in the case of the yeast (*Candida albican*) where all samples showed a versatile inhibition ranging from no inhibition when samples zeolite nanoparticles and nano-zeolite@LDH were applied at low concentration (125ug/l) to maximum inhibition (21 mm) in case of using sample zeolite nanoparticles at a concentration of 1000 ug/l. Closely related to each other, the gram-positive cocci (*Staphylococcus aureus* and *Sarcina lutea*) and the gram-positive rod (*Listeria monocytogenes*) were insensitive to all samples at all concentrations except for *Sarcina lutea* which was sensitive to samples LDH and nano-zeolite@LDH and reached its maximum inhibition when using nano-zeolite@LDH at 1000 ug/l (20.5 mm) Results showed lower MIC values in case of gram-negative bacteria and yeast and greater values in case of gram positive bacteria.



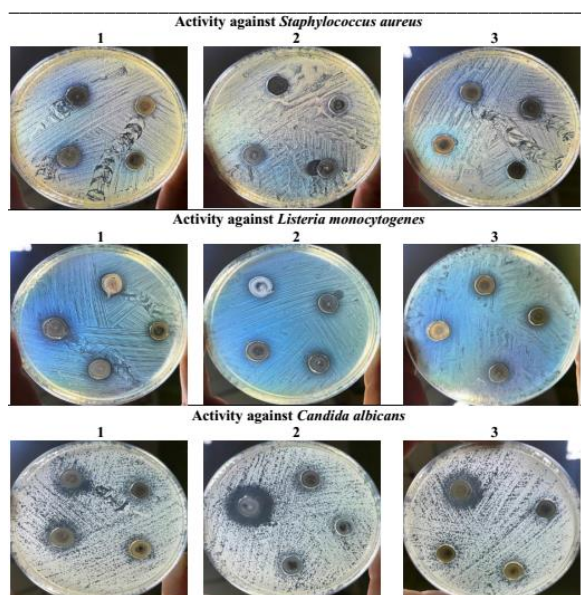


Figure (5) Illustrations showed zone of inhibition caused by FeZn LDH (1), zeolite nanoparticles (2) and nano-zeolite@FeZn LDH (3).

The antimicrobial activity is more evident in gram-negative bacteria than gram-positive bacteria because of the specific structure of the cell wall of gram-positive bacteria which is built of a thick layer of peptidoglycan having a -ve charge that can slow down nanoparticles' actions and make bacteria more resistant [23]. The nanoparticles interact with bacterial cell's basic components such as DNA, lysosomes, ribosomes, and enzymes hence may lead to increase the oxidative stress, protein deactivation, and changes in gene expression [24–25]. The inhibition of *Candida albicans* may be related to membrane damage and inhibition of the normal budding process and destruction of membrane integrity [26].

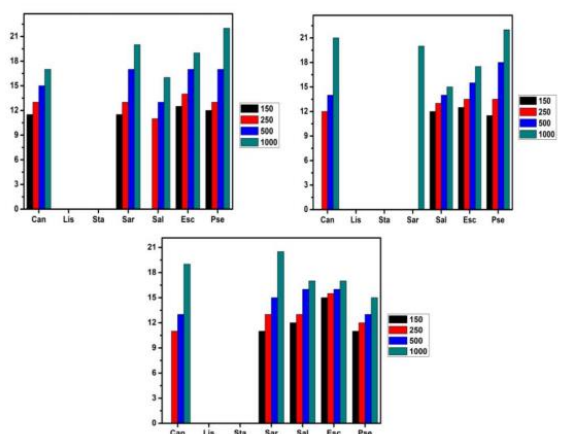


Figure (6) Graphical representation of disc method of inhibition of (a) FeZn LDH, (b) zeolite nanoparticles and (c) nano-zeolite@FeZnLDH against different microbes.

4. Conclusion

In the present work, nano zeolites, FeZn LDH and LDH-zeolite composite were synthesized and characterized. The characterization revealed a high degree of crystallinity as well as a lamellar structure. The nano zeolites, Zn-Fe LDH and Zeolite/LDH

composite were used for significant antibacterial activity when used for gram-positive, gram-negative bacteria, and a fungal strain. The antimicrobial activity is more evident in gram-negative than gram-positive bacteria due to the structure of the cell wall of gram-positive bacteria. This work successfully represents the synthesized materials as antimicrobial materials.

5. Conflicts of interest

“There are no conflicts to declare”.

6. Formatting of funding sources

No funding

7. Acknowledgments

We thank God who gave us the strength to complete this work

8. References

- [1] Xu ZP, Zhang J, Adebajo MO, Zhang H, Zhou C. Catalytic applications of layered double hydroxides and derivatives. *Appl Clay Sci*, 53(2), (2011), 139–50.
- [2] Choy J-H, Choi S-J, Oh J-M, Park T. Clay minerals and layered double hydroxides for novel biological applications. *Appl Clay Sci*, 36(1–3), (2007), 122–132.
- [3] Ziegler C, Werner S, Bugnet M, Wörsching M, Duppl V, Botton GA, et al. Artificial solids by design: Assembly and electron microscopy study of nanosheet-derived heterostructures. *Chem Mater*, 25(24), (2013), 4892–4900.
- [4] Batt AL, Bruce IB, Aga DS. Evaluating the vulnerability of surface waters to antibiotic contamination from varying wastewater treatment plant discharges. *Environ Pollut*, 142(2), (2006), 295–302.
- [5] Kümmerer K. The presence of pharmaceuticals in the environment due to human use—present knowledge and future challenges. *J Environ Manage*, 90(8), (2009), 2354–2366.
- [6] Diaz-Cruz MS, de Alda MJL, Barcelo D. Environmental behavior and analysis of veterinary and human drugs in soils, sediments and sludge. *TrAC Trends Anal Chem*, 22(6), (2003), 340–351.
- [7] Zaher A, Taha M, Mahmoud RK. Possible adsorption mechanisms of the removal of tetracycline from water by Layered Zn-Fe-layered double hydroxide. *J Mol Liq*, 322, (2021), 114546.
- [8] Zhu HY, Orthman JA, Li J-Y, Zhao J-C, Churchman GJ, Vansant EF. Novel composites of TiO₂ (anatase) and silicate nanoparticles. *Chem Mater*, 14(12), (2002), 5037–5044.
- [9] Singh M, Singh S, Prasad S, Gambhir IS. Nanotechnology in medicine and antibacterial effect of silver nanoparticles. *Dig J Nanomater Biostructures*, 3(3), (2008), 115–122.
- [10] Hajipour MJ, Fromm KM, Ashkarran AA, de Aberasturi DJ, de Larramendi IR, Rojo T, et al. Antibacterial properties of nanoparticles. *Trends Biotechnol*, 30(10), (2012), 499–511.
- [11] Azam A, Ahmed AS, Oves M, Khan MS, Habib SS, Memic A. Antimicrobial activity of metal oxide nanoparticles against Gram-positive and Gram-negative bacteria: a comparative study. *Int J Nanomedicine*, 7, (2012), 6003.
- [12] Zaher A, Taha M, Farghali AA, Mahmoud RK. Zn/Fe LDH as a clay-like adsorbent for the removal of oxytetracycline from water: combining experimental results and molecular simulations to understand the removal mechanism. *Environ Sci Pollut Res*. 27(11), (2020), 2256–2269.
- [13] Zhang X, Gao J, Lei Y, Xu Z, Xia S, Jiang Y, et al. Phosphorus removal and mechanisms by Zn-layered double hydroxide (Zn-LDHs)-modified zeolite substrates in a constructed rapid infiltration system. *Rsc Adv*, 9(68), (2019), 39811–39823.

- [14] Gupta NK, Saifuddin M, Kim S, Kim KS. Microscopic, spectroscopic, and experimental approach towards understanding the phosphate adsorption onto Zn–Fe layered double hydroxide. *J Mol Liq*,297, (2020),111935.
- [15] Kamaşoğlu K, Aksoy EA, Akata B, Hasirci N, Baç N. Preparation and characterization of antibacterial zeolite–polyurethane composites. *J Appl Polym Sci*, 110(5), (2008), 2854–2861.
- [16] Babaei M, Anbia M, Kazemipour M. Synthesis of zeolite/carbon nanotube composite for gas separation. *Can J Chem*.95(2), (2017), 162–168.
- [17] Gamil S, El Rouby WMA, Antuch M, Zedan IT. Nanohybrid layered double hydroxide materials as efficient catalysts for methanol electrooxidation. *RSC Adv*, 9(24), (2019), 13503–13514.
- [18] Gao Y, Ru Y, Zhou L, Wang X, Wang J. Preparation and characterization of chitosan-zeolite molecular sieve composite for ammonia and nitrate removal. *Adv Compos Lett*,27(5), (2018), 096369351802700502.
- [19] Prasetyo TAB, Soegijono B. Characterization of sonicated natural zeolite/ferric chloride hexahydrate by infrared spectroscopy. In: *Journal of Physics: Conference Series. IOP Publishing*,(2018), p. 12022.
- [20] Saraya ME, Thabet MS. Characterization and evaluation of natural zeolite as a pozzolanic material. *Al-Azhar Bull Sci*, 29(1-A), (2018), 17–34.
- [21] Elkartehi ME, Mahmoud R, Shehata N, Farghali A, Gamil S, Zaher A. LDH Nanocubes Synthesized with Zeolite Templates and Their High Performance as Adsorbents. *Nanomaterials*, 11(12),(2021),3315.
- [22] Domínguez AV, Algaba RA, Canturri AM, Villodres ÁR, Smani Y. Antibacterial activity of colloidal silver against gram-negative and gram-positive bacteria. *Antibiotics*, 9(1), (2020).
- [23] Shrivastava S, Bera T, Roy A, Singh G, Ramachandrarao P, Dash D. Characterization of enhanced antibacterial effects of novel silver nanoparticles. *Nanotechnology*, 18(22),(2007), 225103.
- [24] Yang W, Shen C, Ji Q, An H, Wang J, Liu Q, et al. Food storage material silver nanoparticles interfere with DNA replication fidelity and bind with DNA. *Nanotechnology*, 20(8),(2009), 85102.
- [25] Xu Y, Wei M-T, Ou-Yang HD, Walker SG, Wang HZ, Gordon CR, et al. Exposure to TiO₂ nanoparticles increases *Staphylococcus aureus* infection of HeLa cells. *J Nanobiotechnology*, 14(1), (2016),1–16.
- [26] Nasrollahi, A., K. H. Pourshamsian, and P. Mansourkiaee. Antifungal activity of silver nanoparticles on some of fungi. *Int.J.Nano.Dim*,1(3),(2011), 233-239.